Critical Reviews in Biochemistry and Molecular Biology, 2011; 46(2): 152–164

ISSN 1040-9238 print/ISSN 1549-7798 online
DOI: 10.3109/10409238.2011.559451

informa
healthcare

REVIEW ARTICLE

Protein-nucleic acid complexes and the role of mass spectrometry in their structure determination

Ah Young Park and Carol V. Robinson

Department of Chemistry, University of Oxford, South Parks Road, Oxford, UK

Abstract

Mass spectrometry is now established as a powerful tool for the study of the stoichiometry, interactions, dynamics, and subunit architecture of large protein assemblies and their subcomplexes. Recent evidence has suggested that the 3D structure of protein complexes can be maintained intact in the gas phase, highlighting the potential of ion mobility to contribute to structural biology. A key challenge is to integrate the compositional and structural information from ion mobility mass spectrometry with molecular modelling approaches to produce 3D models of intact protein complexes. In this review, we focus on the mass spectrometry of protein-nucleic acid assemblies with particular attention to the application of ion mobility, an emerging technique in structural studies. We also discuss the challenges that lie ahead for the full integration of ion mobility mass spectrometry with structural biology.

Keywords: Mass spectrometry; ion-mobility mass spectrometry; collision cross section; structural biology; hybrid structure determination

Introduction

Essential cellular functions are carried out by networks of interacting proteins that exist in large dynamic and heterogeneous assemblies. Understanding the interactions within these assemblies is vital to understanding the function of the cell. Many structural studies focus on well-defined stable cores for high-resolution structure determination, primarily by X-ray crystallography. For intact protein assemblies, much insight has been gained from electron microscopy (EM); however, it is often difficult to assign subunits within EM density maps due to the relatively low resolution that is attained. Mass spectrometry (MS) has become a powerful adjunct to structural biology since the introduction of soft ionization techniques, specifically electrospray (ES), and specialized instrumentation that maintains noncovalent interactions of large protein complexes (Sobott et al., 2002a; Hernández and Robinson, 2007).

Since noncovalent interactions can be maintained, MS in theory, offers a powerful approach for establishing the integrity of the several hundred putative protein complexes proposed from tandem-affinity purification (TAP) and proteomic studies of budding yeast (Gavin et al., 2006). Although the composition of these complexes was determined from standard proteomics techniques, subunit interaction maps and topological restraints were not defined. MS of an intact complex isolated via TAP can characterize its heterogeneity, composition, and stoichiometry (Hernández et al., 2006; Figure 1). Subunit interaction maps are then obtained by generating overlapping subcomplexes, primarily using solution phase disruption techniques. Gas-phase dissociation processes, however, in general, lead to the unfolding of a peripheral subunit (Jurchen and Williams, 2003; Benesch, 2009; Boeri Erba et al., 2010; Pagel et al., 2010). Tandem MS enables selection and interrogation of individual charge states in a mass spectrum (Figure 1). Therefore, it allows the unambiguous identification of mass and composition of a subcomplex or complex of interest.

Extensive information on interaction networks can be obtained from mild in-solution disruption of the intact complex. By carefully adjusting ionic strength, pH or addition of various organic solvents, hydrophilic or hydrophobic interactions between subunits can be

Address for Correspondence: Carol V. Robinson, Department of Chemistry, University of Oxford, South Parks Road, Oxford, OX1 3QZ, UK. E-mail: carol.robinson@chem.ox.ac.uk

(Received 29 November 2010; revised 28 January 2011; accepted 28 January 2011)

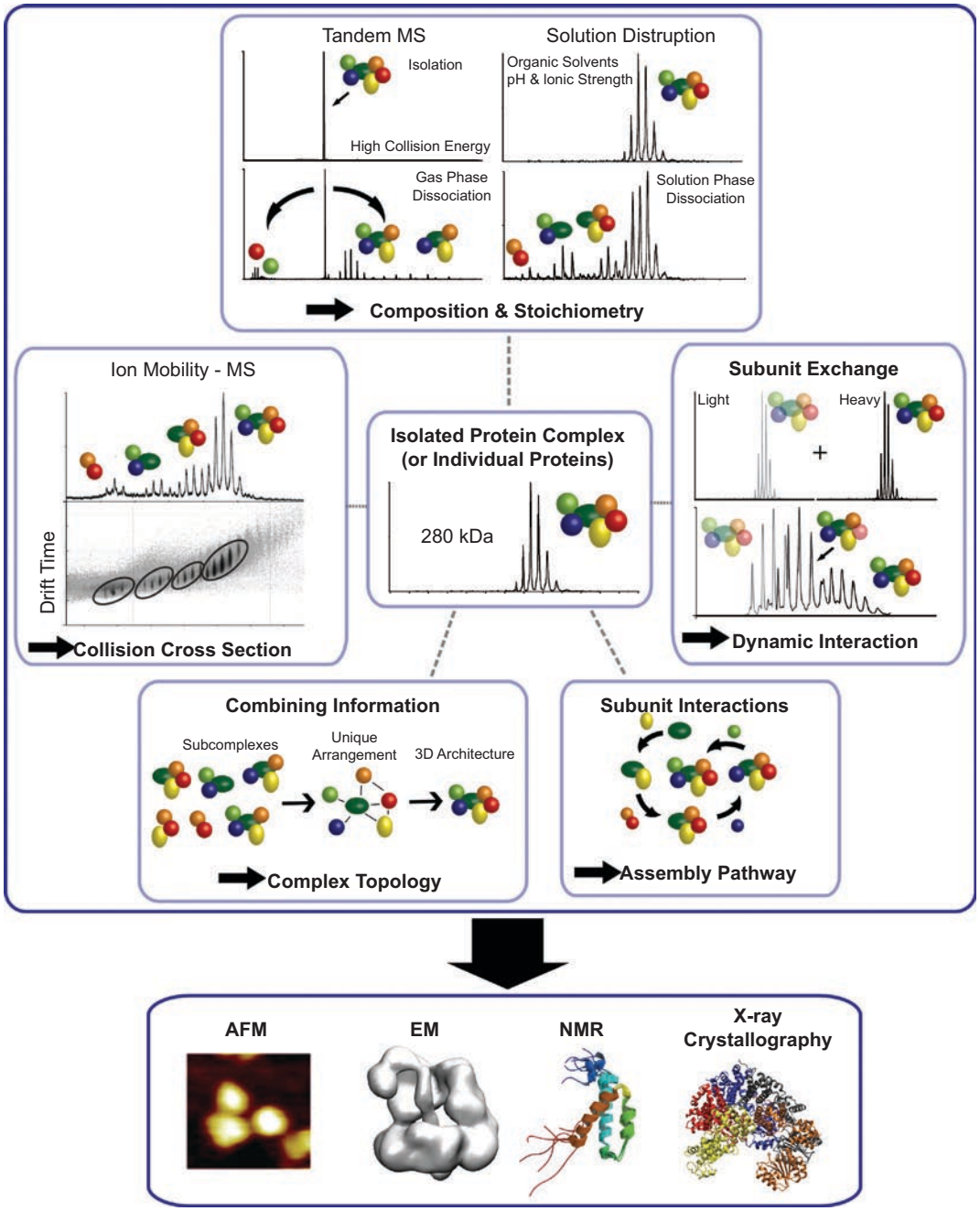

Figure 1. General introduction to mass spectrometry (MS) and ion mobility (IM)-MS, and their application in structural biology. From either an isolated protein complex or individual proteins, MS and IM-MS enable determination of the (i) composition and stoichiometry of protein subunits, (ii) dynamic interactions involving the exchange of protein subunits, (iii) the assembly pathway of a complex from individual subunits or subcomplexes, (iv) the overall topology and arrangement of subunits, and (v) the collision cross sections of complex or protein ions. Considering each aspect in turn, (i) Composition and stoichiometry of the protein complex can be determined following either gas-phase or solution-phase disruption techniques. In the gas phase, tandem MS allows isolation of a peak of interest which is subsequently subjected to gas-phase activation. This leads to unfolding of a peripheral subunit of the protein complex, which dissociates leaving a "stripped" subcomplex. For solution-phase disruption, addition of small quantities of organic solvent or adjusting the pH or ionic strength of the complex-containing solution typically generates subcomplexes. (ii) Dynamics within the protein complex can be monitored by the exchange of protein subunits between complexes. In general, labelled proteins (heavy which maybe either "tagged" or labelled isotopically) are incubated with unlabelled proteins (light) and the composition of the intact complex is observed as a function of time. (iii) The assembly pathway of a protein complex can be determined by introducing proteins individually or in combination to explore the subunit interactions of stable intermediate subcomplexes. (iv) An interaction map can be constructed from subcomplexes identified by tandem MS after solution disruption experiments leading to the determination of its 3D architecture. (v) The collision cross section is determined from the drift time of ions separated according to their transmission through a gas-filled mobility cell. Larger ions travel more slowly than smaller ions, resulting in longer drift times. All the information gathered from these MS and IM-MS approaches contributes to other structural biology techniques to enable so-called "hybrid" structure determination (Robinson et al., 2007). AFM, atomic force microscopy (Thirlway et al., 2004); EM, electron microscopy (Mayanagi et al., 2009); NMR, nuclear magnetic resonance (Keniry et al., 2006); and X-ray crystallography (Jeruzalmi et al., 2001).-

disrupted (Figure 1; Hernández et al., 2006; Hernández and Robinson, 2007; Levy et al., 2008; Zhou et al., 2008; Sharon et al., 2009). As such, the nature and strength of subunit interfaces within an intact complex can be inferred. From the information gathered from both gas-phase and solution dissociation experiments, the connectivity map can be drawn using suitable software packages (e.g., SUMMIT; Taverner et al., 2008). This algorithm uses an exhaustive search for masses that sum to the target mass over all allowed stoichiometries within a given error range and draws the shortest network pathway that connects all subunits with their interaction partners.

Given the ability to maintain interactions in protein assemblies in the gas phase (Loo, 1997; Ashcroft, 2005; Sharon and Robinson, 2007; Heck, 2008), MS offers an opportunity to monitor directly the assembly pathway from component subunits as well as the real-time dynamics of subunit exchange (Figure 1; Sobott et al., 2002b; Painter et al., 2008). For the analysis of assembly pathways, component subunits can be introduced either individually or in combination to probe the stable intermediate subcomplexes. For subunit exchange experiments, the composition of the intact complex is monitored as a function of time after incubation of complexes with isotopically labelled proteins or subunits with sequence modifications or mass tags. This approach allows extraction of real-time kinetics and subunit exchange mechanisms (Aquilina et al., 2005; Keetch et al., 2005; Hyung et al., 2010; Smith et al., 2010).

Over the past few years, ion mobility mass spectrometry (IM-MS) has emerged as an effective means of studying the overall topology of multiprotein complexes (Figure 1; Loo et al., 2005; Kaddis et al., 2007; Ruotolo et al., 2008; Uetrecht et al., 2010). Application of IM-MS has been rapidly increasing since the introduction of commercially available instrumentation (Pringle et al., 2007). In most ion mobility experiments, ions are separated in a cell, filled with neutral gas, and subjected to a weak electric field. Large ions undergo more collisions with neutral gas and travel more slowly than smaller ions, giving rise to longer drift times. Changes in drift time can be indicative of conformational changes in protein complexes, for example, in response to ligand binding (Ruotolo et al., 2005). After careful calibration, drift times are converted to collision cross sections (CCS), which are averaged over all possible orientations of ions. The CCS value is then compared with a theoretically calculated CCS produced for a series of trial structures, generated by molecular modelling and calculated using the program MOBCAL (Mesleh et al., 1996). The detailed protocol for data collection and interpretation of MS and ion mobility data are described elsewhere (Ruotolo et al., 2008; Scarff et al., 2008; Smith et al., 2009). Accumulating evidence suggests that a protein complex in the gas phase under appropriate conditions can preserve their overall topology in the absence of bulk solvent. This suggests great promise for the application of IM-MS in structural biology (Ruotolo et al., 2005; Lorenzen et al., 2008; Uetrecht et al., 2008; Pukala et al., 2009; van Duijn et al., 2009).

In this review, we discuss the application of MS and IM-MS, focussing on protein machines that function with nucleic acids. We begin by reviewing one of the first investigations of the potential of IM-MS for maintaining the topology of a protein-nucleic acid complex in the gas phase. Using the well-characterized complex, the *trp* RNA binding attenuation protein (TRAP), its overall topology was explored in *apo* and *holo* forms, revealing that its characteristic ring-shaped topology can be preserved in the mass spectrometer (Ruotolo et al., 2005). Following this study, different recombinant subunits are used to probe the assembly pathway and dynamics of the clamp loader of the *Escherichia coli* DNA replicase (Park et al., 2010). Subsequently, the conformational changes within the clamp loader were probed using IM-MS (Politis et al., 2010). More heterogeneous are the endogenous RNA polymerase complexes. We review MS studies of the stoichiometry and composition of yeast RNA polymerase II and present a 3D model structure of the initiation heterotrimer of RNA polymerase III constrained by CCS analysis (Lane et al., 2011). Related to these RNA polymerase studies, we describe recent progress in deciphering a subunit interaction map for a coactivator of the RNA polymerase, the mediator complex. Focussing on the middle module of the complex, the authors investigate interaction modules as well as their overall topology and conformational heterogeneity (Koschubs et al., 2010). Building on the theme of complexity and dynamics, we review the total interaction map of the 13-subunit eukaryotic initiation factor 3 complex (eIF3), isolated directly from HeLa cells while associated to the human 40S ribosomal subunit. We show how subunit interaction data can be fitted into EM density maps, guided by CCS analysis of different heteromers and "footprinting" of an internal ribosome entry site RNA (Zhou et al., 2008).

All of the protein-nucleic acid complexes described in this review have different levels of structural information, from complete and incomplete atomic structures through to low-resolution EM density maps with no high-resolution structural data. Many are complicated by their inherent heterogeneity and dynamics. Consequently, these protein-nucleic acid systems serve to illustrate the role of MS and IM-MS when applied in combination with X-ray crystallography, computational modeling, and cryo-electron microscopy. Specifically, we show how this so-called hybrid structural approach (Robinson et al., 2007) can reveal new insights into the structure and function of complex protein-nucleic acid machineries.

Evidence for protein structure in the gas phase

Many examples have been reported in which subunit interactions within a protein complex can survive in gas phase. Until recently, however, it was unclear whether these gas-phase complexes could maintain their overall topology in the absence of bulk water. To assess the topology of a protein complex with a well-defined 3D structure,

the TRAP complex was studied by IM-MS (Ruotolo et al., 2005). TRAP assembles into a well-characterized oligomer with eleven ~8 kDa subunits in a ring topology. The structure was established from X-ray analysis of TRAP in the presence of tryptophan (Antson et al., 1995, 1999) and the mechanism of tryptophan binding to TRAP was established by MS (McCammon et al., 2004). In the mass spectrum of *apo* TRAP, four charge states are observed (Figure 2A). Arrival time distributions for each charge state were recorded and then converted to CCS. The lowest charge (19+) has a value that is in close agreement with the value calculated from the X-ray structure (6600 Å^2). The 20+ charge state has a bimodal distribution, indicating retention of some native-like structure together with buckling of the ring (Figure 2C top). Stability of TRAP increases upon tryptophan binding (Antson et al., 1999) but little change is observed in the mass spectrum, and the maximum CCS measured remains constant between the *apo* and Trp-bond forms. This is expected since tryptophan associates between TRAP subunits. However, the bimodal distribution observed for the *apo* form is no longer observed, reflecting an increase in the stability of the ring structure (Figure 2C middle). It has also been established that binding a 53-base segment of the *trp* leader mRNA in the presence of tryptophan stabilizes the TRAP complex (McCammon et al., 2004). A 12% increase in the overall CCS of TRAP in the presence of RNA and tryptophan is observed in comparison with *apo* TRAP (Figure 2B and 2C bottom). Since RNA binding at an internal site would add only marginally to the overall CCS of TRAP, this increase implies that RNA binds to the periphery of the protein complex, increasing the CCS as would be anticipated from the X-ray structure. Structural heterogeneity detected for *apo* TRAP is not observed for the TRAP-tryptophan-RNA complex, in agreement with the rigidity of the ring structure conferred by RNA binding. This study opened up a myriad of applications of IM-MS for studying structural changes within protein complexes.

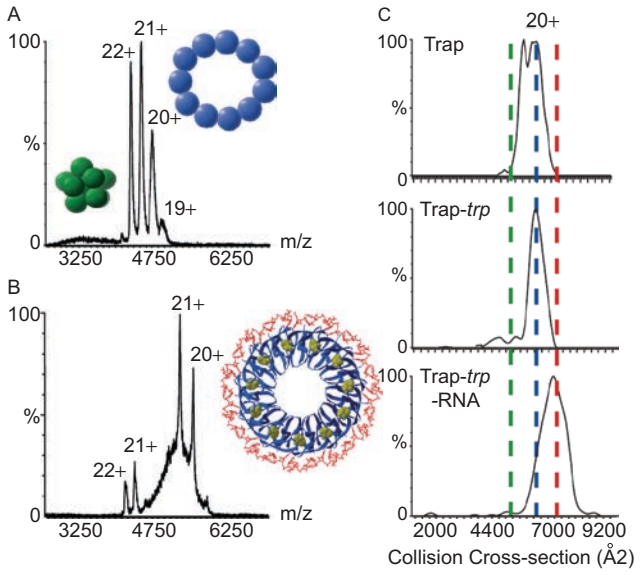

Figure 2. IM-MS data for the *trp* RNA binding attenuation protein (TRAP) complex in the presence and absence of ligands. Mass spectra of *apo*-TRAP (A) and TRAP-RNA-tryptophan (B) and IM data for the 20+ ion of *apo*-TRAP (top), TRAP-tryptophan (middle), and TRAP-RNA-tryptophan (bottom) are shown (C). Two model structures of TRAP (ring and collapsed ring) are represented in blue and green, respectively, in a space-filling representation. The collision cross sections (CCS) values corresponding for the two models are shown in blue and green dashed line. The red dashed line represents CCS of the TRAP-RNA-tryptophan crystal structure. The crystal structure of the TRAP-RNA-tryptophan complex (PDB ID: 1C9S; Antson et al., 1995) is illustrated using the program SIB Swiss PDB viewer (blue: TRAP, red: trphytophan, and silver: RNA).

Defining assembly, dynamics, and subunit architecture

Many structural and biochemical techniques rely on highly homogenous soluble protein subunits in relatively high concentrations. While these properties are also advantageous for MS, only a few micro-liters of micromolar protein concentration are required, once appropriate buffer conditions are identified (Hernández and Robinson, 2007). This means that many different reactions can be investigated without large consumption of protein. This property was used to good effect in a recent investigation of the assembly of the clamp loader complex involved in DNA replication (Park et al., 2010). The DNA polymerase III (Pol III) holoenzyme is part of the replication machinery. One of its three subassemblies, the clamp loader complex, is responsible for loading/unloading of another subassembly, the β_2 sliding clamp (Naktinis et al., 1995; Johnson and O'Donnell, 2005; Schaeffer et al., 2005). The clamp loader complex is composed of seven subunits: three of either τ, γ or δ, δ', ψ and χ. $(\tau/\gamma)_3\delta\delta'$ which form a central ring that performs the central ATPase activity (Dallmann and McHenry, 1995). The peripheral ψχ heterodimer connects the clamp loader complex with other subunits within the holoenzyme (Xiao et al., 1993a, 1993b). Unusually, τ and γ are translated from the same gene, *dnaX*, and share the same three N-terminal domains that are essential for the clamp loader (Tsuchihashi and Kornberg, 1990). Recombinant expression of all six proteins enabled a comprehensive evaluation of the assembly mechanism through the analysis of many different subunit combinations.

The composition of the clamp complex was deduced by X-ray crystallography of the $\gamma_3\delta\delta'$ ring. Previous studies had suggested that τ/γ exist in both monomeric and tetrameric forms, interestingly not as a trimer (Dallmann and McHenry, 1995). Therefore, the mechanism by which monomers and tetramers of τ/γ, in the presence of δδ', were converted into trimers was ambiguous. Mass spectra of individual recombinant subunits of τ and γ confirmed that both τ and γ exist predominately as tetramers, in equilibrium with monomers and also dimers and trimers (Figure 3A). In a systematic investigation of interactions among the components of the clamp

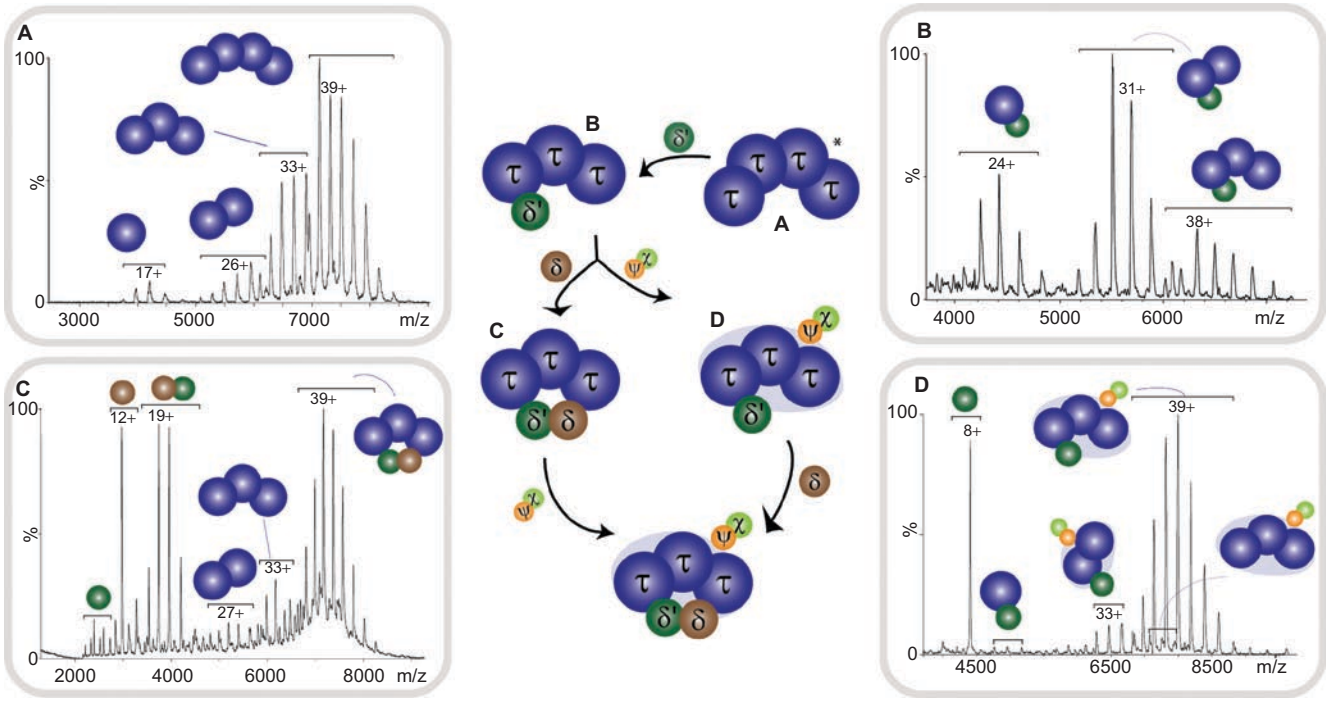

Figure 3. Assembly pathway of the clamp loader revealed by MS. Each individual subunit of the *E. coli* clamp loader complex, $\tau_3\delta\delta'\psi\chi$ was subjected to analysis of the assembly pathway. (A) τ exists predominantly as tetramers and (B) δ' initiates the assembly by dissociating τ tetramers into smaller oligomeric units. (C and D) Both δ and ψχ interact with the τδ' subcomplexes, resulting in either $\tau_3\delta\delta'$ or $\tau_3\delta'\psi\chi$. Further addition of ψχ and δ leads to the full assembly of clamp loader, $\tau_3\delta\delta'\psi\chi$.

loader, δ' was identified as an initiator that dissociates the τ/γ tetramer into smaller oligomeric species (Figure 3B). Only after association of δ' can δ bind and stabilize the trimeric form of τ/γ, thus completing the pentameric ring of $(\tau/\gamma)_3\delta\delta'$ (Figure 3C). The ψχ heterodimer further ensures the correct stoichiometry of τ/γ by stabilizing the τ/γ trimers in the presence of δ' (Figure 3D).

One of the great advantages of MS is the rapid time frame for recording spectra, enabling observation of dynamic and transient interactions in real time (Sharon and Robinson, 2007). In particular, monitoring subunit exchange can determine kinetics of the assembly processes (Hyung et al., 2010). This can be readily achieved by exchanging a subunit with a subunit that differs in mass but with identical structural properties (e.g., isotopically labelled or tagged). As mentioned above, τ and γ share three identical domains that associate with δδ' to assemble the clamp loader complex. Therefore, all forms of $(\tau/\gamma)_3\delta\delta'$ can function as the clamp loader. However, at least two τ subunits are required in the clamp loader complex to bind to the polymerase and helicase during DNA replication. Since both τ and γ are synthesized from the same gene, it is interesting to consider how cells avoid clamp loaders with less than two τ subunits during replication. MS is ideally placed to investigate this question using subunit exchange experiments.

Equimolar solutions of τ and γ complexes were allowed to exchange subunits in the absence of other proteins. The resulting mass spectra recorded after various time intervals showed that all five possible tetrameric species (τ_4, $\tau_3\gamma$, $\tau_2\gamma_2$, $\tau\gamma_3$, and γ_4) were formed rapidly within the dead time of the experiment and in a statistical distribution (Figure 4A). However, in the presence of δδ', exchange occurs on a much longer time scale (Figure 4B). Interestingly, this exchange is slower than the time required for chromosome replication (~40 min). As a consequence, although all forms of the clamp loader complex exist in cells, once the replisome is formed, with either $\tau_3\delta\delta'$ or $\tau_2\gamma\delta\delta'$, further exchange of τ and γ is prevented. Consequently, while considerable structural information is available for this complex, these subunit exchange experiments enable an investigation of the dynamics of the assembly process.

High-resolution atomic coordinates of the γ complex have been reported (Jeruzalmi et al., 2001). However, large sections of the protein sequence are not present in these structures. Moreover, structures of the individual subunits of γ and δ have not been determined. From the assembly pathway, it was suggested that δ' serves as the anchor that stabilizes the flexible γ and δ subunits. To investigate any conformational changes in individual subunits, with or without δ', 'IM-MS was applied (Politis et al., 2010). All three subunits are related and have three similar domains although only γ can bind ATP. Interestingly, little difference was observed for the X-ray structures of δ' within the γ complex and in isolation, indicating structural rigidity in δ' (Guenther et al., 1997; Jeruzalmi et al., 2001). Furthermore, the experimental CCS value of the individual δ' subunits corresponded well with the X-ray structure (Jeruzalmi

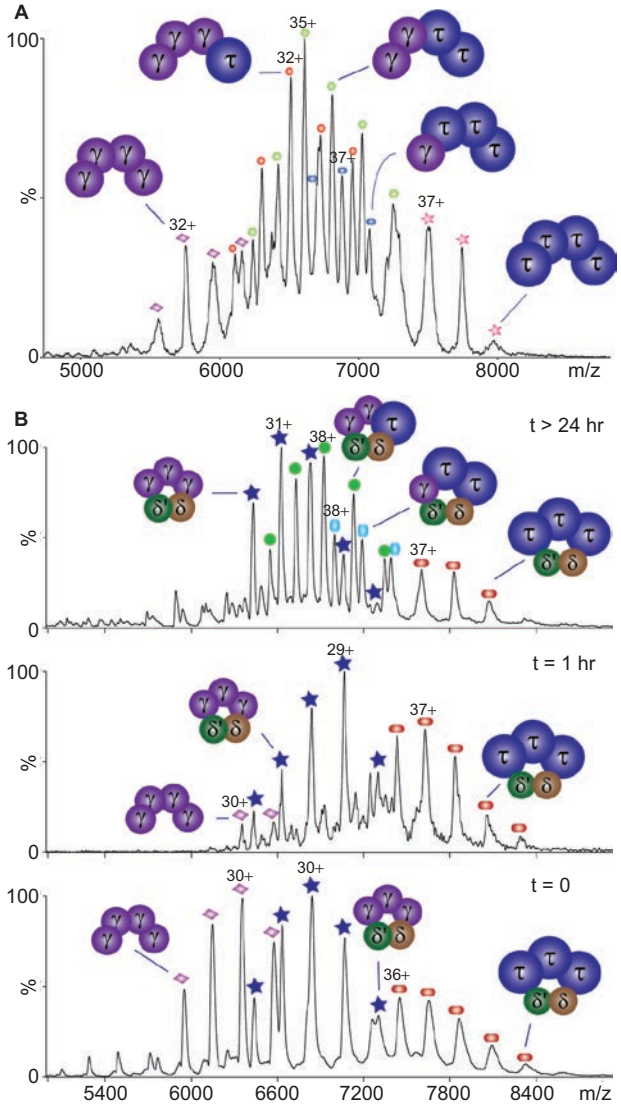

Figure 4. Subunit exchange dynamics between τ and γ. (A) Mass spectra of τ and γ show rapid subunit exchange between the subunits as all five possible tetrameric species (τ_4, $\tau_3\gamma$, $\tau_2\gamma_2$, $\tau\gamma_3$, and γ_4) are observed within the dead time of the experiment (<15 s) at 0°C. (B) With δδ', the subunit exchange between τ and γ is considerably slower. Mass spectra of $\tau_3\delta\delta'$ in the presence of γ_4 obtained at different time intervals. At $t=0$, free δδ' interacts with γ_4 rapidly and forms the $\gamma_3\delta\delta'$ complex (bottom spectrum). Middle spectrum ($t=1$ h) shows low-intensity peaks (not labelled), which increase in intensity after 24 h (top spectrum). All four possible complexes were identified $\tau_3\delta\delta'$, $\tau_2\gamma\delta\delta'$, $\tau\gamma_2\delta\delta'$, and $\gamma_3\delta\delta'$.

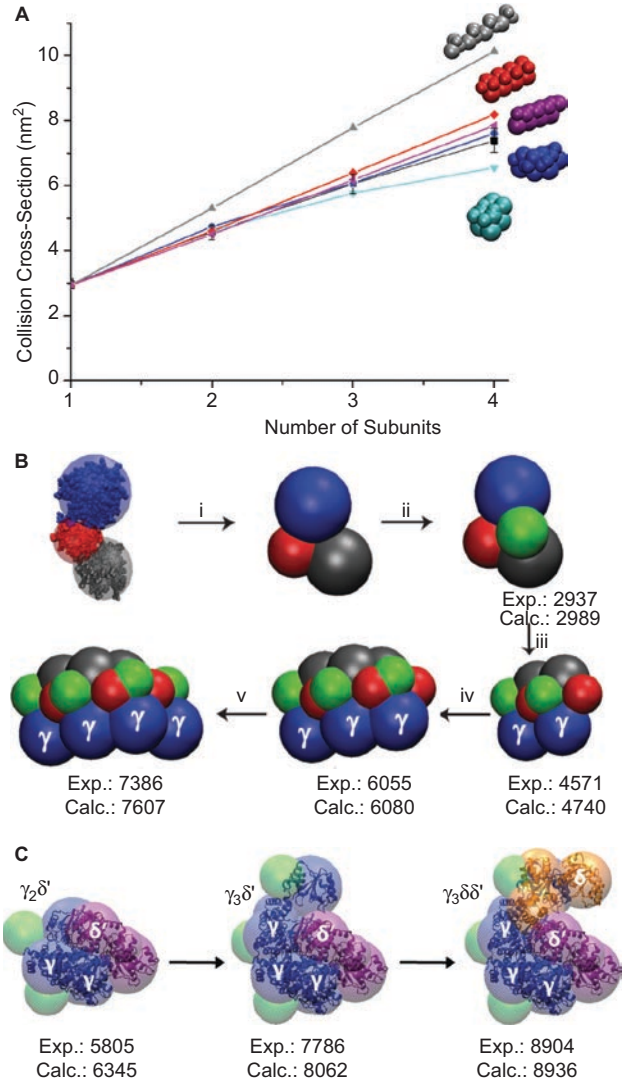

Figure 5. Architecture of the γ complex and its subunits based on IM-MS. (A) Archetypal geometries of the γ oligomers presented according to CCS. Experimental CCS values of the γ oligomers are shown in black. The compact arrangement mined from the atomic structure of γ in the crystal structure of $\gamma_3\delta\delta'$ is shown in blue and provided the closest to the experimental CCS. (B) Building the γ oligomers sequentially, starting from the full length γ monomer based on the crystal structure (i–ii) and higher oligomeric species of γ (iii–v). (i) CG model of γ was represented with three spheres, corresponding to each domain. (ii) a model of γ in a more compact form. (C) CG model structures for $\gamma_2\delta'$, $\gamma_3\delta'$, and $\gamma_3\delta\delta'$ complexes. The experimental CCS (Exp) and theoretically calculated CCS of a model (Calc) are shown in Å².

et al., 2001). In contrast, CCS values that are 10% lower than calculated were observed for γ and δ, even when taking into account residues that are absent from the structure. This indicates that γ and δ adopt compact conformations in contrast to δ'. Model structures of compact γ oligomers are assembled by using a coarse-grained (CG) approach (Figure 5A and 5B). In this case, the three domains of γ was represented as overlapping spheres to generate models of γ that include residues not present in the X-ray structure. These compact conformations maybe attributed to the innate flexibility in γ and δ, important for their catalytic activity in the γ complex.

The role of δ' was rationalized as the provider of the static interface for γ and δ and to confer stability to the γ complex. This speculation was further supported by model structures built for the $\gamma_3\delta'$ and $\gamma_2\delta'$ subcomplexes, taking into account residues not present in γ (~13%)(Figure 5c). These models were consistent with the tertiary structure of γ being maintained as seen in the X-ray structure. The full model structure of the γ complex also suggested that

γ and δ no longer adopt a compact conformation in the presence of δ'. These results show the applicability of combining modeling and IM-MS to elucidate structural changes during heterocomplex assembly.

Identifying stable modules and structural flexibility

RNA polymerases transcribe DNA into RNA, are essential to life and conserved through all organisms. Three different types of RNA polymerases (I, II, and III) exist in eukaryotes and are responsible for synthesizing rRNA, mRNA, and tRNA, respectively. RNA polymerases share many similarities in their stable cores. RNA Pol I and III contain additional subunits that confer differences in their specificity and functionality. Detailed structural and functional analysis of RNA Pol II has contributed to a basic framework for understanding other polymerases (Armache et al., 2003; Kettenberger et al., 2003; Armache et al., 2005; Cramer et al., 2008; Kostrewa et al., 2009). However, complexity and heterogeneity in RNA Pol I and Pol III have hindered high-resolution structural studies and only cryo-EM reconstructions are available to date (Fernández-Tornero et al., 2007; Kuhn et al., 2007).

RNA Pol III is the most complex polymerase of the three, comprising 17 subunits with a molecular weight of around 700 kDa. In comparison, Pol I and II consist of 14 and 12 subunits with molecular masses of ~600 and 500 kDa, respectively. Five subunits unique to RNA Pol III form two subcomplexes, C53/C37 and C31/C82/C34. The C53/C37 heterodimer is involved in termination and together with C11, re-initiation downstream of the DNA (Landrieux et al., 2006). The C31/C82/C34 heterotrimer has a number of roles including transcriptional initiation of tRNA, unwinding of the dsDNA and open complex formation, and recognition of the transcription factor (TF) IIIB (Werner et al., 1992; Bartholomew et al., 1993; Thuillier et al., 1995; Brun et al., 1997; Wang and Roeder, 1997). However, it remains unclear how the specific subunits are arranged and assembled with respect to the structural core of the 12 subunits of Pol II.

MS of endogenous RNA Pol III purified from yeast cells identified an intact complex with 17 subunits (Lorenzen et al., 2007; Lane et al., 2011). In addition, minor species of Pol III in the absence of two subunits, C53 and C37, were observed, indicating the peripheral position of the two subunits. By tagging C53, the C53/C37 heterodimer was isolated and its ease of dissociation from the core suggested that the C-terminus of C53, where the TAP tag is located, contacts the core. The labile association of C53/C37 fits its role in recognizing terminator elements in Pol III and is consistent with its peripheral location identified in EM studies (Fernández-Tornero et al., 2007).

Subassemblies of RNA Pol III were generated at high pH and include the stable C31/C82/C34 heterotrimer, the C82/C31, and C25/C17 heterodimers as well as many individual subunits, ABC10α, ABC23, C11, C82, and C34 (Figure 6A). To investigate the topological arrangement of C31/C82/C34 heterotrimer, the recombinant complex was produced and subjected to high salt solution conditions to determine subunit connectivity. Two heterodimers, C82/C31 and C82/C34, were observed. C31/C34 was not observed under any conditions, suggesting a linear arrangement of C31/C82/C34 with C82 bridging C31 and C34. This observation was in contrast to the C31/C34 interaction deduced from yeast two-hybrid assays (Flores et al., 1999) and an alternative linear arrangement of C31/C34/C82 proposed previously (Lorenzen et al., 2007).

The reconstituted transcription bubble readily associates with RNA Pol III. A remarkably well-resolved mass spectrum was recorded, the major species corresponding to the elongation complex that includes the entire complex with that transcription bubble (Figure 6B). Interestingly, the initiation trimer, C31/C82/C34, leaves the enlongation complex more easily than from the *apo* form. This could be a result of the transcription bubble weakening the interaction between the trimer and the core complex. This observation corresponds well with the roles of the translation trimer described above.

In the absence of any high-resolution structural information at the subunit level, it is difficult to integrate IM-MS data into modelling for large hetro-complexes. Therefore, the CG approach outlined above is most suitable for modelling unknown structures. IM-MS analysis of the C31/C82/C34 heterotrimer and subsequent building of modules (C31/C82, C82/C34, C34, and C82) led to a CG model of the heterotrimer (Figure 6C). Initially, each subunit was represented as either one or two spheres depending on its mass and shape within the EM density (Fernández-Tornero et al., 2007; Pukala et al., 2009; Politis et al., 2010). The relative position and overlap between the subunits was defined by the experimental CCS of C31/C82 and C82/C34. The model was placed within the density difference between the EM structure of Pol III (Fernández-Tornero et al., 2007) and the crystal structure of Pol II (Cramer et al., 2001; Figure 6C). A considerable surface area of the trimer is revealed by this model which may be related to its functional role of binding additional factors and DNA, bringing them to the polymerase core.

For the RNA polymerases, the crystal structure of the core aids interpretation of the data for RNA Pol III. However much less structural information is available for the Mediator complex, the central coactivator required for regulated transcription by RNA Pol II (Björklund and Gustafsson, 2005; Kornberg, 2005). The Mediator complex consists of 25 subunits, divided into four structural modules: head, middle, tail, and kinase. In a recent MS study, the recombinant complete seven-subunit middle module (Med1:4:7:9:10:21:31) was observed along with six (Med4:7:9:10:21:31) and four (Med7:10:21:31) subunit subcomplexes (Koschubs et al., 2010). Subsequent loss of Med1, Med4:9 indicated the peripheral position of these subunits. Adding small amounts of organic solvents, DMSO, or n-propanol further dissociated these assemblies. For the six-subunit subassembly, the Med4:9 dimer was isolated, confirming direct interaction between these two subunits. Dissociation of the four-subunit complex

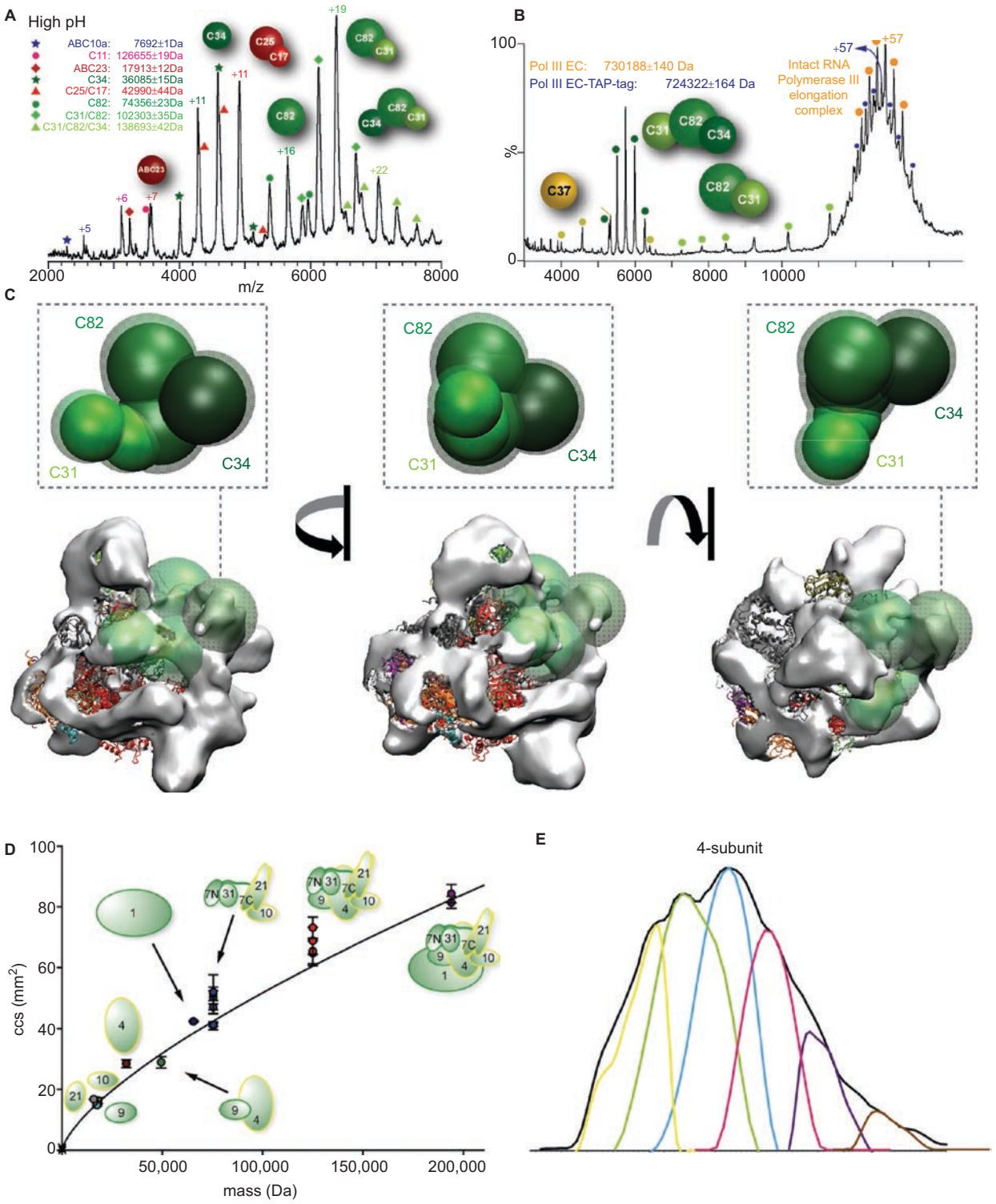

Figure 6. Mass spectra and model structures of the RNA Pol III subcomplexes and IM-MS analysis of the middle module of the Mediator complex. (A) Mass spectrum of RNA Pol III at high pH (30% v/v ammonium hydroxide at pH 10.9) shows dissociation of subunits (ABC10a, ABC23, C34, and C82) and subcomplexes (C25/C17, C82/C31, and C34/C82/C31). (B) Mass spectrum of RNA Pol III elongation complex shows the intact complex with the transcriptional bubble and additional labile subcomplexes, C82/C31 and C34/C82/C31. (C) A CG model of the C34/C82/C31 trimer is shown in three orthogonal orientations. C34 was represented as a single sphere in comparison with two overlapping spheres representing multiple domains in C82 and C31. Experimental error (~5%) was accounted for in the model as the shaded area. A model was placed in the density difference between the EM map of Pol III and the crystal structure of Pol II (ribbon diagram, PDB code: 1 WCM; Armache et al., 2005). (D) The experimental CCS values of subunit and (sub-) complexes of the Mediator middle module are plotted against their masses. The general trend of CCS versus mass for globular proteins is shown as a solid line. (E) The arrival time distribution of the four-subunit subassembly Med 7:10:21:31 is shown. Up to six different conformations of the subassembly were detected, indicated by six colored lines.

produced several trimers and dimers; only the Med7 subunit was present in every complex. This result suggested that Med7 is a central subunit of the middle module of the Mediator complex and enabled a preliminary subunit interaction map to be deduced.

In order to provide structural information, IM-MS analysis of subunits, subassemblies, and the complete middle module were obtained. (Figure 6D). The experimental CCS was then compared with the CCS of globular proteins. Many individual subunits fit the description of globular proteins. For the four- and six-subunit complexes, conformational flexibility of the middle module of the Mediator complex was apparent from drift time analysis. For the four-subunit complex, the drift times suggested up to six different conformations. Interestingly, the six-subunit complex has a more elongated conformation than the seven-subunit complex of the middle module. The inherent flexibility observed by IM-MS provides a rational for the difficulties encountered in obtaining X-ray analysis of this complex. More generally, this study demonstrates applicability of IM-MS in capturing the dynamic topological nature of protein complexes.

Piecing together a three-dimensional interaction map

Heteromeric protein complexes in theory can provide the most detailed interaction maps. Particularly advantageous is a diversity of subunit masses and many subcomplexes. This combination enables assembly of numerous interacting modules which, if there are a sufficiently high number, could allow for a unique arrangement and pseudo 3D network. An example of this approach is the eIF3, purified directly from HeLa cells on the side of the 40S subunit (Siridechadilok et al., 2005; Damoc et al., 2007). Eukaryotic initiation factors mediate mRNA binding to the 40S ribosomal subunit before assembly of active ribosomes for protein synthesis. eIF3 consists of 13 different subunits and is the largest translation initiation factor (~800 kDa; Hinnebusch, 2006). Due to its likely heterogeneity and dynamics, no high-resolution structure is available but an EM density map defines an irregular particle with five distinct appendages (Siridechadilok et al., 2005).

Despite the heterogeneity of the complex, remarkably well-resolved mass spectra show a homogeneous population of eIF3 with all 13 different subunits present (a, b, c, d, e, f, g, h, I, j, k, l, and m; Figure 7A). The peripheral subunits of eIF3i, j, k, and l were tentatively assigned by their ready dissociation in tandem MS. Overlapping intact subassemblies of eIF3 were then characterized by varying the ionic strength of the buffer (Figure 7B). Three structural modules, eIF3(i:g), eIF3(e:l:k), and eIF3(f:h:m), were readily observed. At different ionic strength, various large subcomplexes were isolated, eIF3(c:d:e:l:k) and eIF3(a:b:i:g) which are linked by interactions between subunits b and c. Using all the information gathered from both the solution- and gas-phase dissociation experiments, supplemented with immunoprecipitation results, a connectivity map was deduced using the software package SUMMIT (Taverner et al., 2008). The final model of the human eIF3, derived from 27 subcomplexes, is consistent with previous studies of the mammalian eIF3 functional core which contains subunits a, b, c, e, f, and h (Masutani et al., 2007). The MS study shows how the additional subunits, present in the human eIF3, assemble into subcomplexes and associate with this stable core (Zhou et al., 2008).

The virus Internal Ribosome Entry Site (IRES) RNA targets eIF3 for an alternative initiation pathway for protein synthesis. The mass spectrum of eIF3 in the presence of the hepatitis C virus (HCV) IRES RNA shows an increase in m/z, compared with eIF3 alone (Figure 7C and 7D). The resolution of the peaks of the eIF3-IRES RNA binary complex is compromised due to the introduction of RNA in the binding buffer which contains magnesium. Nonetheless, comparison between activated mass spectra of eIF3 and eIF3-IRES RNA demonstrates that the large subcomplexes are no longer formed while eIF3i and the i:k dimer persist. This result indicates that IRES RNA binds and stabilizes the large subcomplexes formed with core subunits but does not affect the small peripheral subcomplexes.

For eIF3, three subassemblies are frequently observed under the high-ionic strength conditions. These include two heterotrimers (f:h:m and e:l:k) and one heterodimer (l:k; Figure 7B). Interestingly, for f:h:m, all possible dimers (f:h, h:m, and f:m) were readily observed, indicating that f:h:m has a trigonal geometry wherein all three subunits interact. In contrast, only two dimers (e:l and l:k) are observed for the e:l:k trimer, suggesting a linear arrangement. Interestingly, despite the higher mass of f:h:m, the average CCS recorded was much lower than e:l:k (5545 and 6677 Å^2, respectively; Figure 8A). This suggests that f:h:m adopts a more compact arrangement compared with e:l:k.

To model the structural arrangement of both heterotrimers, each subunit is modelled initially as a sphere where the radius is related to the mass of the subunit. Assuming the overlap between the subunits is similar in both subassemblies, two models were constructed (Figure 8B). The calculated CCS of the elongated model of f:h:m is much higher than the observed CCS (green dashed line, Figure 8B, top panel) but is in excellent agreement with the trigonal arrangement. By contrast, the calculated CCS of the compact trigonal model for e:l:k is much lower than the observed CCS (blue dashed line, Figure 8B, bottom panel) but is consistent with an extended linear arrangement. Comparison with the EM density map determined for this complex strongly suggests that the subcomplex e:l:k occupies the extended linear density (Figure 8C). F:h:m is likely to occupy the lower right appendage. This study demonstrates the power of IM-MS not only to define a series of subcomplexes but also to constrain them by their CCS and subsequently to fit them into an EM density map.

Summary and future perspectives

It is now established that MS can unravel the composition, stoichiometry, heterogeneity, dynamics, and

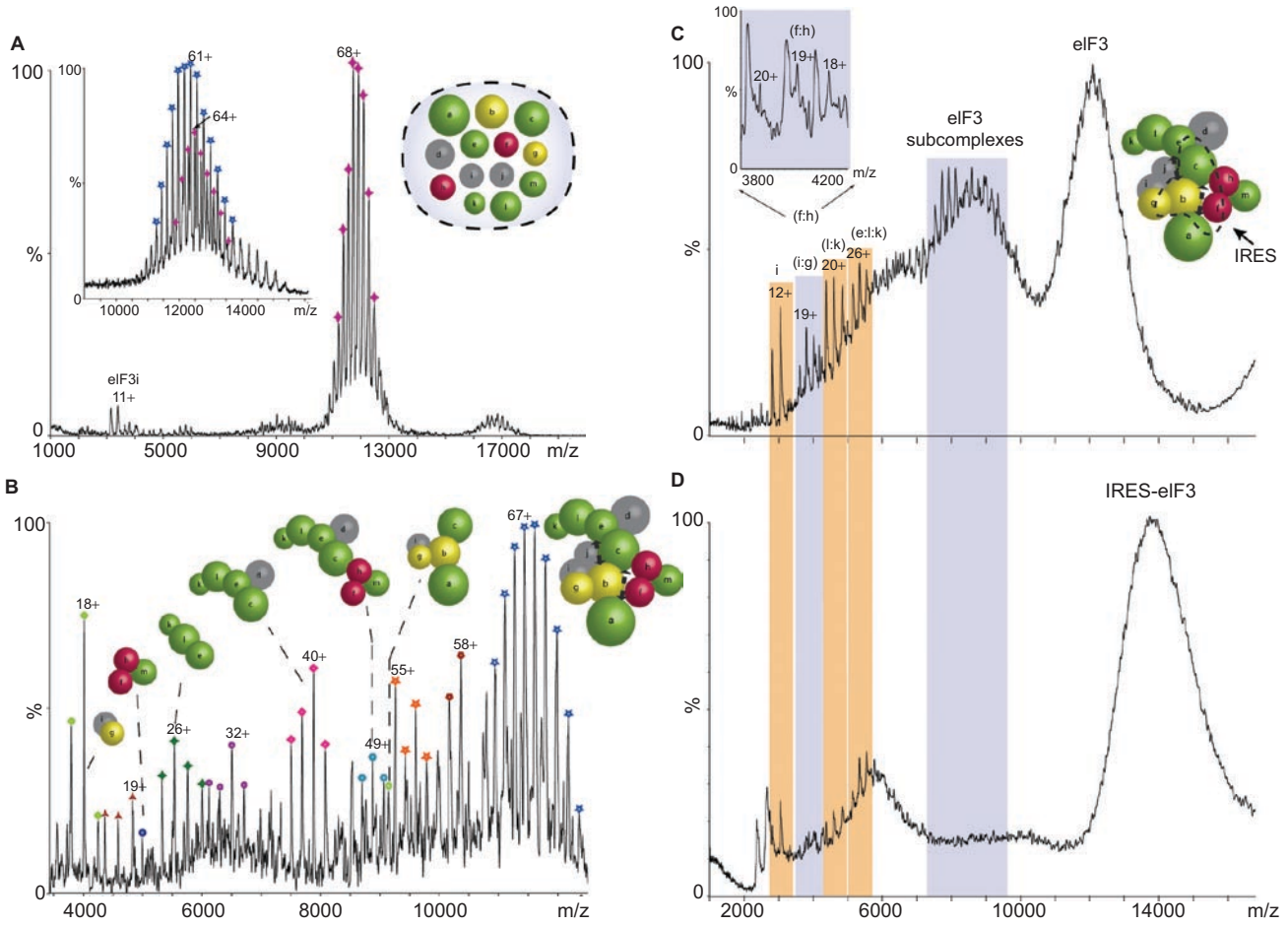

Figure 7. A complete subunit interaction map of human eukaryotic initiation factor 3 (eIF3) revealed by MS. (A) Mass spectrum of the intact eIF3 complex composed of 13 subunits. Each subunit is represented as a scaled circle according to its mass. Subunits containing PCI (Proteasome, COP9, eIF3), MPN (Mpr1-Pad1 N-terminal) domains, RNA recognition motifs, or no common domains are shown in green, red, yellow, or gray, respectively. (Inset) Mass spectrum of eIF3 at high energy, showing an additional charge state series that corresponds to eIF3 with dissociated eIF3j (blue star). (B) Mass spectrum of eIF3 under intermediate ionic strength buffer (350 mM AmAc). Using tandem MS, 27 subcomplexes of human eIF3 were identified and a model architecture was derived from additional data from immunoprecipitation and interactions identified in the yeast complex. Arrows represent contacts observed which cannot be represented in this model. Mass spectra of eIF3 (C) in the presence of hepatitis C virus (HCV)-Internal Ribosome Entry Site (IRES) (D) under the same condition. Binding of IRES to eIF3 results in a shift in *m/z* value but some peaks are no longer resolved. Dissociation of the i subunit, l:k, and e:l:k subcomplexes are not affected by IRES binding (in orange). In contrast, peaks corresponding i:g and f:h dimers are greatly decreased and subcomplexes observed in eIF3 are not present in the presence of IRES(in blue). Subunits that are influenced by interaction with IRES are shown within the dashed line.

interaction maps of protein complexes (Loo, 1997; Sharon and Robinson, 2007; Heck, 2008; Zhou and Robinson, 2010). Combined with IM, another dimension of information, the CCS, can be obtained. In this review, we focussed on the application of MS and IM-MS to four large protein complexes that function in DNA and RNA replication and translation. Many attributes of the MS-only approach are illustrated by this series of four complexes including a broad mass range (up to a few MDa), low sample consumption (microlitre quantities at low micromolar concentration), rapid collection and analysis of data (minutes to hours), and the ability to observe conformational and compositional heterogeneity. To these properties, IM data are able to contribute important conformational dynamics, as in the γ complex and the middle module of the mediator complex. It is also able to constrain three-dimensional models for subcomplexes, enabling their fitting into EM density maps as was shown for the yeast Pol III and human eIF3.

These IM-MS approaches, for protein-nucleic acid complexes, are however still in development with many challenges remaining. Improved accuracy in CCS measurements for protein complexes was demonstrated recently with the publication of a large database of absolute CCS values. This included many protein complexes and confirmed the importance of employing native-like protein complexes for accurate and reliable CCS measurements (Bush et al., 2010). Another limiting factor is the IM resolution that affects the analysis of heterogeneous protein complexes. In addition to these practical considerations of paramount importance is the need for a systematic approach to integrate IM-MS data with existing structural data. Preliminary approaches are emerging that combine incomplete atomic

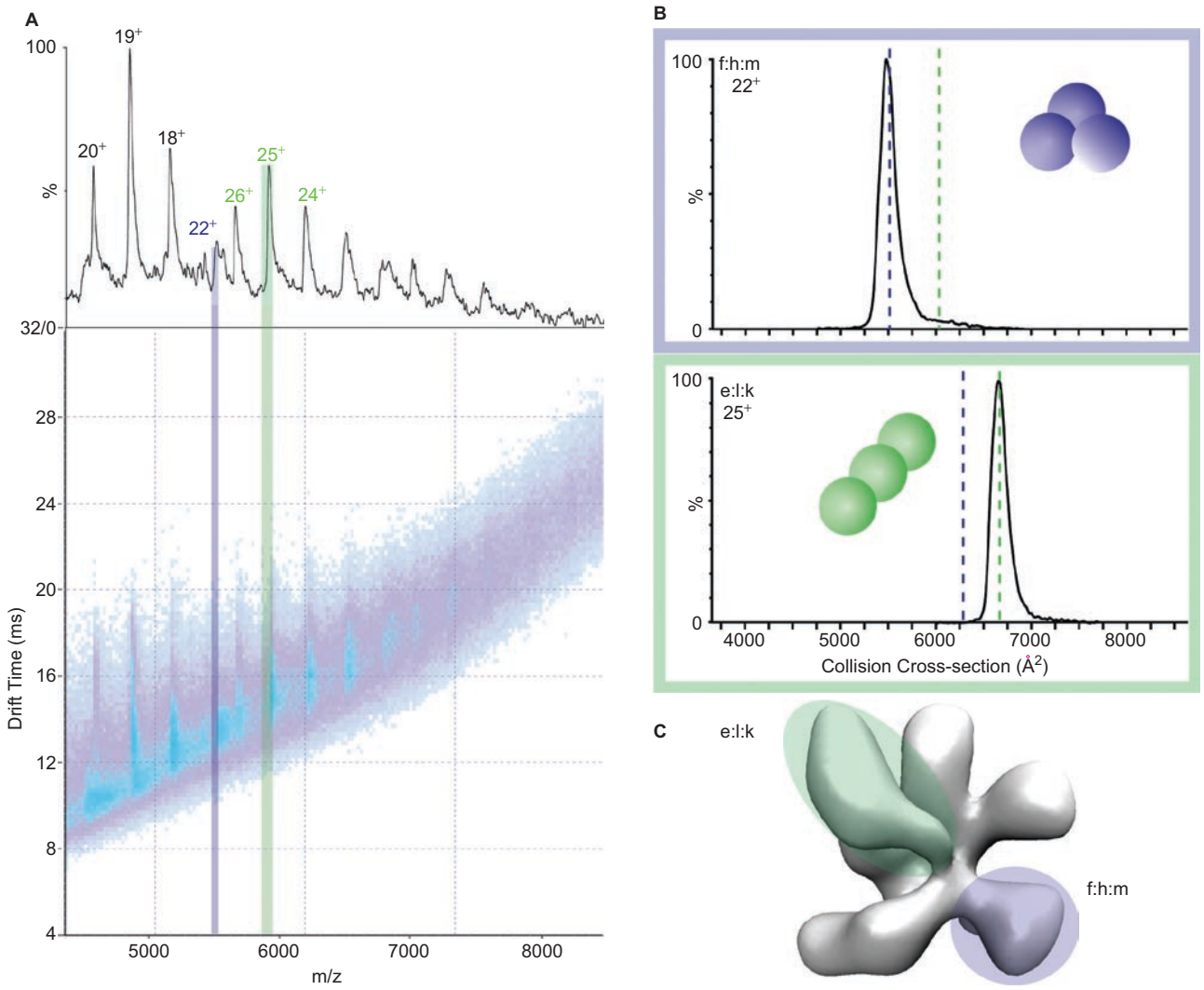

Figure 8. IM-MS data used to determine the topology of eIF3 subcomplexes and their location within the EM density. (A) Mass spectrum and drift time versus *m/z* contour plot are shown for the eIF3 subcomplexes of e:l:k, f:h:m, and l:k. Charge states of the subcomplexes are assigned in green, purple, and black, respectively. (B) Arrival time distribution converted to CCS are shown for the two trimeric complexes, f:h:m and e:l:k. A close-packed trimer of f:h:m and an elongated trimer of e:l:k was predicted. (C) Two trimers are shown in the context of the EM map of eIF3.

structures and CCS values to provide complete models of multiprotein complexes (Politis et al., 2010).

As the protein-nucleic acid complexes of interest become ever more challenging in terms of their size, complexity, and abundance, it is important to bring to the fore all methods that contribute to their structure determination in so-called "hybrid" structural methods (Robinson et al., 2007). The methods described in this review provide one such hybrid approach. With the information that can be obtained from these MS techniques, it is possible to define both the composition and topology of interacting modules and consequently to contribute to the overall 3D structure of key protein-nucleic acid complexes.

Declaration of interest

We acknowledge funding from the BBSRC (to A.Y.P.) and the Royal Society (to C.V.R.).

References

Antson AA, Otridge J, Brzozowski AM, Dodson EJ, Dodson GG, Wilson KS, Smith TM, Yang M, Kurecki T, Gollnick P. 1995. The structure of trp RNA-binding attenuation protein. Nature 374:693–700.

Antson AA, Dodson EJ, Dodson G, Greaves RB, Chen X, Gollnick P. 1999. Structure of the trp RNA-binding attenuation protein, TRAP, bound to RNA. Nature 401:235–242.

Aquilina JA, Benesch JL, Ding LL, Yaron O, Horwitz J, Robinson CV. 2005. Subunit exchange of polydisperse proteins: mass spectrometry reveals consequences of alphaA-crystallin truncation. J Biol Chem 280:14485–14491.

Armache KJ, Kettenberger H, Cramer P. 2003. Architecture of initiation-competent 12-subunit RNA polymerase II. Proc Natl Acad Sci USA 100:6964–6968.

Armache KJ, Mitterweger S, Meinhart A, Cramer P. 2005. Structures of complete RNA polymerase II and its subcomplex, Rpb4/7. J Biol Chem 280:7131–7134.

Ashcroft AE. 2005. Recent developments in electrospray ionisation mass spectrometry: noncovalently bound protein complexes. Nat Prod Rep 22:452–464.

Bartholomew B, Durkovich D, Kassavetis GA, Geiduschek EP. 1993. Orientation and topography of RNA polymerase III in transcription complexes. Mol Cell Biol 13:942–952.

Benesch JL. 2009. Collisional activation of protein complexes: picking up the pieces. J Am Soc Mass Spectrom 20:341–348.

Björklund S, Gustafsson CM. 2005. The yeast Mediator complex and its regulation. Trends Biochem Sci 30:240–244.

Boeri Erba E, Ruotolo BT, Barsky D, Robinson CV. 2010. Ion mobility-mass spectrometry reveals the influence of subunit packing and charge on the dissociation of multiprotein complexes. Anal Chem 82:9702–9710.

Brun I, Sentenac A, Werner M. 1997. Dual role of the C34 subunit of RNA polymerase III in transcription initiation. EMBO J 16:5730–5741.

Bush MF, Hall Z, Giles K, Hoyes J, Robinson CV, Ruotolo BT. 2010. Collision cross sections of proteins and their complexes: a calibration framework and database for gas-phase structural biology. Anal Chem 82:9557–9565.

Cramer P, Bushnell DA, Kornberg RD. 2001. Structural basis of transcription: RNA polymerase II at 2.8 angstrom resolution. Science 292:1863–1876.

Cramer P, Armache KJ, Baumli S, Benkert S, Brueckner F, Buchen C, Damsma GE, Dengl S, Geiger SR, Jasiak AJ, Jawhari A, Jennebach S, Kamenski T, Kettenberger H, Kuhn CD, Lehmann E, Leike K, Sydow JF, Vannini A. 2008. Structure of eukaryotic RNA polymerases. Annu Rev Biophys 37:337–352.

Dallmann HG, McHenry CS. 1995. DnaX complex of Escherichia coli DNA polymerase III holoenzyme. Physical characterization of the DnaX subunits and complexes. J Biol Chem 270:29563–29569.

Damoc E, Fraser CS, Zhou M, Videler H, Mayeur GL, Hershey JW, Doudna JA, Robinson CV, Leary JA. 2007. Structural characterization of the human eukaryotic initiation factor 3 protein complex by mass spectrometry. Mol Cell Proteomics 6:1135–1146.

Fernández-Tornero C, Böttcher B, Riva M, Carles C, Steuerwald U, Ruigrok RW, Sentenac A, Müller CW, Schoehn G. 2007. Insights into transcription initiation and termination from the electron microscopy structure of yeast RNA polymerase III. Mol Cell 25:813–823.

Flores A, Briand JF, Gadal O, Andrau JC, Rubbi L, Van Mullem V, Boschiero C, Goussot M, Marck C, Carles C, Thuriaux P, Sentenac A, Werner M. 1999. A protein-protein interaction map of yeast RNA polymerase III. Proc Natl Acad Sci USA 96:7815–7820.

Gavin AC, Aloy P, Grandi P, Krause R, Boesche M, Marzioch M, Rau C, Jensen LJ, Bastuck S, Dümpelfeld B, Edelmann A, Heurtier MA, Hoffman V, Hoefert C, Klein K, Hudak M, Michon AM, Schelder M, Schirle M, Remor M, Rudi T, Hooper S, Bauer A, Bouwmeester T, Casari G, Drewes G, Neubauer G, Rick JM, Kuster B, Bork P, Russell RB, Superti-Furga G. 2006. Proteome survey reveals modularity of the yeast cell machinery. Nature 440:631–636.

Guenther B, Onrust R, Sali A, O'Donnell M, Kuriyan J. 1997. Crystal structure of the delta' subunit of the clamp-loader complex of E. coli DNA polymerase III. Cell 91:335–345.

Heck AJ. 2008. Native mass spectrometry: a bridge between interactomics and structural biology. Nat Methods 5:927–933.

Hernández H, Dziembowski A, Taverner T, Séraphin B, Robinson CV. 2006. Subunit architecture of multimeric complexes isolated directly from cells. EMBO Rep 7:605–610.

Hernández H, Robinson CV. 2007. Determining the stoichiometry and interactions of macromolecular assemblies from mass spectrometry. Nat Protoc 2:715–726.

Hernández H, Makarova OV, Makarov EM, Morgner N, Muto Y, Krummel DP, Robinson CV. 2009. Isoforms of U1-70k control subunit dynamics in the human spliceosomal U1 snRNP. PLoS ONE 4:issue 9, e7202, 2009.

Hinnebusch AG. 2006. eIF3: a versatile scaffold for translation initiation complexes. Trends Biochem Sci 31:553–562.

Hyung SJ, Deroo S, Robinson CV. 2010. Retinol and retinol-binding protein stabilize transthyretin via formation of retinol transport complex. ACS Chem Biol 5:1137–1146.

Jeruzalmi D, O'Donnell M, Kuriyan J. 2001. Crystal structure of the processivity clamp loader gamma (gamma) complex of E. coli DNA polymerase III. Cell 106:429–441.

Johnson A, O'Donnell M. 2005. Cellular DNA replicases: components and dynamics at the replication fork. Annu Rev Biochem 74:283–315.

Jurchen JC, Williams ER. 2003. Origin of asymmetric charge partitioning in the dissociation of gas-phase protein homodimers. J Am Chem Soc 125:2817–2826.

Kaddis CS, Lomeli SH, Yin S, Berhane B, Apostol MI, Kickhoefer VA, Rome LH, Loo JA. 2007. Sizing large proteins and protein complexes by electrospray ionization mass spectrometry and ion mobility. J Am Soc Mass Spectrom 18:1206–1216.

Keetch CA, Bromley EH, McCammon MG, Wang N, Christodoulou J, Robinson CV. 2005. L55P transthyretin accelerates subunit exchange and leads to rapid formation of hybrid tetramers. J Biol Chem 280:41667–41674.

Keniry MA, Park AY, Owen EA, Hamdan SM, Pintacuda G, Otting G, Dixon NE. 2006. Structure of the theta subunit of Escherichia coli DNA polymerase III in complex with the epsilon subunit. J Bacteriol 188:4464–4473.

Kettenberger H, Armache KJ, Cramer P. 2003. Architecture of the RNA polymerase II-TFIIS complex and implications for mRNA cleavage. Cell 114:347–357.

Kornberg RD. 2005. Mediator and the mechanism of transcriptional activation. Trends Biochem Sci 30:235–239.

Koschubs T, Lorenzen K, Baumli S, Sandström S, Heck AJ, Cramer P. 2010. Preparation and topology of the Mediator middle module. Nucleic Acids Res 38:3186–3195.

Kostrewa D, Zeller ME, Armache KJ, Seizl M, Leike K, Thomm M, Cramer P. 2009. RNA polymerase II-TFIIB structure and mechanism of transcription initiation. Nature 462:323–330.

Kuhn CD, Geiger SR, Baumli S, Gartmann M, Gerber J, Jennebach S, Mielke T, Tschochner H, Beckmann R, Cramer P. 2007. Functional architecture of RNA polymerase I. Cell 131:1260–1272.

Landrieux E, Alic N, Ducrot C, Acker J, Riva M, Carles C. 2006. A subcomplex of RNA polymerase III subunits involved in transcription termination and reinitiation. EMBO J 25:118–128.

Lane LA, Fernández-Tornero C, Zhou M, Morgner N, Ptchelkine D, Steuerwald U, Politis A, Lindner D, Gvozdenovic J, Gavin AC, Müller CW, Robinson CV. 2011. Mass spectrometry reveals stable modules in holo and apo RNA polymerases I and III. Structure 19:90–100.

Levy ED, Boeri Erba E, Robinson CV, Teichmann SA. 2008. Assembly reflects evolution of protein complexes. Nature 453:1262–1265.

Loo JA. 1997. Studying noncovalent protein complexes by electrospray ionization mass spectrometry. Mass Spectrom Rev 16:1–23.

Loo JA, Berhane B, Kaddis CS, Wooding KM, Xie Y, Kaufman SL, Chernushevich IV. 2005. Electrospray ionization mass spectrometry and ion mobility analysis of the 20S proteasome complex. J Am Soc Mass Spectrom 16:998–1008.

Lorenzen K, Vannini A, Cramer P, Heck AJ. 2007. Structural biology of RNA polymerase III: mass spectrometry elucidates subcomplex architecture. Structure 15:1237–1245.

Lorenzen K, Olia AS, Uetrecht C, Cingolani G, Heck AJ. 2008. Determination of stoichiometry and conformational changes in the first step of the P22 tail assembly. J Mol Biol 379:385–396.

Masutani M, Sonenberg N, Yokoyama S, Imataka H. 2007. Reconstitution reveals the functional core of mammalian eIF3. EMBO J 26:3373–3383.

Mayanagi K, Kiyonari S, Saito M, Shirai T, Ishino Y, Morikawa K. 2009. Mechanism of replication machinery assembly as revealed by the DNA ligase-PCNA-DNA complex architecture. Proc Natl Acad Sci USA 106:4647–4652.

McCammon MG, Hernández H, Sobott F, Robinson CV. 2004. Tandem mass spectrometry defines the stoichiometry and quaternary structural arrangement of tryptophan molecules in the multiprotein complex TRAP. J Am Chem Soc 126:5950–5951.

Mesleh MF, Hunter JM, Shvartsburg AA, Schatz GC, Jarrold MF. 1996. Structural information from ion mobility measurements: effects of the long-range potential. J Phys Chem 100:16082–16086.

Naktinis V, Onrust R, Fang L, O'Donnell M. 1995. Assembly of a chromosomal replication machine: two DNA polymerases, a clamp loader, and sliding clamps in one holoenzyme particle. II. Intermediate complex between the clamp loader and its clamp. J Biol Chem 270:13358–13365.

Pagel K, Hyung SJ, Ruotolo BT, Robinson CV. 2010. Alternate dissociation pathways identified in charge-reduced protein complex ions. Anal Chem 82:5363–5372.

Painter AJ, Jaya N, Basha E, Vierling E, Robinson CV, Benesch JL. 2008. Real-time monitoring of protein complexes reveals their quaternary organization and dynamics. Chem Biol 15:246–253.

Park AY, Jergic S, Politis A, Ruotolo BT, Hirshberg D, Jessop LL, Beck JL, Barsky D, O'Donnell M, Dixon NE, Robinson CV. 2010. A single subunit directs the assembly of the Escherichia coli DNA sliding clamp loader. Structure 18:285–292.

Politis A, Park AY, Hyung SJ, Barsky D, Ruotolo BT, Robinson CV. 2010. Integrating ion mobility mass spectrometry with molecular modelling to determine the architecture of multiprotein complexes. PLoS ONE 5:e12080.

Pringle SD, Giles K, Wildgoose JL, Williams JP, Slade SE, Thalassinos K, Bateman RH, Bowers MT& Scrivens JH. 2007. An investigation of the mobility separation of some peptide and protein ions using a new hybrid quadrupole/travelling wave IMS/oa-ToF instrument. Int J Mass Spectrom 261: 1–12.

Pukala TL, Ruotolo BT, Zhou M, Politis A, Stefanescu R, Leary JA, Robinson CV. 2009. Subunit architecture of multiprotein assemblies determined using restraints from gas-phase measurements. Structure 17:1235–1243.

Robinson CV, Sali A, Baumeister W. 2007. The molecular sociology of the cell. Nature 450:973–982.

Ruotolo BT, Giles K, Campuzano I, Sandercock AM, Bateman RH, Robinson CV. 2005. Evidence for macromolecular protein rings in the absence of bulk water. Science 310:1658–1661.

Ruotolo BT, Benesch JL, Sandercock AM, Hyung SJ, Robinson CV. 2008. Ion mobility-mass spectrometry analysis of large protein complexes. Nat Protoc 3:1139–1152.

Scarff CA, Thalassinos K, Hilton GR, Scrivens JH. 2008. Travelling wave ion mobility mass spectrometry studies of protein structure: biological significance and comparison with X-ray crystallography and nuclear magnetic resonance spectroscopy measurements. Rapid Commun Mass Spectrom 22:3297–3304.

Schaeffer PM, Headlam MJ, Dixon NE. 2005. Protein–protein interactions in the eubacterial replisome. IUBMB Life 57:5–12.

Sharon M, Robinson CV. 2007. The role of mass spectrometry in structure elucidation of dynamic protein complexes. Annu Rev Biochem 76:167–193.

Sharon M, Mao H, Boeri Erba E, Stephens E, Zheng N, Robinson CV. 2009. Symmetrical modularity of the COP9 signalosome complex suggests its multifunctionality. Structure 17:31–40.

Siridechadilok B, Fraser CS, Hall RJ, Doudna JA, Nogales E. 2005. Structural roles for human translation factor eIF3 in initiation of protein synthesis. Science 310:1513–1515.

Smith DP, Knapman TW, Campuzano I, Malham RW, Berryman JT, Radford SE, Ashcroft AE. 2009. Deciphering drift time measurements from travelling wave ion mobility spectrometry-mass spectrometry studies. Eur J Mass Spectrom (Chichester, Eng) 15:113–130.

Smith DP, Radford SE, Ashcroft AE. 2010. Elongated oligomers in beta2-microglobulin amyloid assembly revealed by ion mobility spectrometry-mass spectrometry. Proc Natl Acad Sci USA 107:6794–6798.

Sobott F, Hernández H, McCammon MG, Tito MA, Robinson CV. 2002a. A tandem mass spectrometer for improved transmission and analysis of large macromolecular assemblies. Anal Chem 74:1402–1407.

Sobott F, Benesch JL, Vierling E, Robinson CV. 2002b. Subunit exchange of multimeric protein complexes. Real-time monitoring of subunit exchange between small heat shock proteins by using electrospray mass spectrometry. J Biol Chem 277:38921–38929.

Taverner T, Hernández H, Sharon M, Ruotolo BT, Matak-Vinkovic D, Devos D, Russell RB, Robinson CV. 2008. Subunit architecture of intact protein complexes from mass spectrometry and homology modeling. Acc Chem Res 41:617–627.

Thirlway J, Turner IJ, Gibson CT, Gardiner L, Brady K, Allen S, Roberts CJ, Soultanas P. 2004. DnaG interacts with a linker region that joins the N- and C-domains of DnaB and induces the formation of 3-fold symmetric rings. Nucleic Acids Res 32:2977–2986.

Thuillier V, Stettler S, Sentenac A, Thuriaux P, Werner M. 1995. A mutation in the C31 subunit of Saccharomyces cerevisiae RNA polymerase III affects transcription initiation. EMBO J 14:351–359.

Tsuchihashi Z, Kornberg A. 1990. Translational frameshifting generates the gamma subunit of DNA polymerase III holoenzyme. Proc Natl Acad Sci USA 87:2516–2520.

Uetrecht C, Versluis C, Watts NR, Wingfield PT, Steven AC, Heck AJ. 2008. Stability and shape of hepatitis B virus capsids in vacuo. Angew Chem Int Ed Engl 47:6247–6251.

Uetrecht C, Rose RJ, van Duijn E, Lorenzen K, Heck AJ. 2010. Ion mobility mass spectrometry of proteins and protein assemblies. Chem Soc Rev 39:1633–1655.

van Duijn E, Barendregt A, Synowsky S, Versluis C, Heck AJ. 2009. Chaperonin complexes monitored by ion mobility mass spectrometry. J Am Chem Soc 131:1452–1459.

Wang Z, Roeder RG. 1997. Three human RNA polymerase III-specific subunits form a subcomplex with a selective function in specific transcription initiation. Genes Dev 11:1315–1326.

Werner M, Hermann-Le Denmat S, Treich I, Sentenac A, Thuriaux P. 1992. Effect of mutations in a zinc-binding domain of yeast RNA polymerase C (III) on enzyme function and subunit association. Mol Cell Biol 12:1087–1095.

Xiao H, Crombie R, Dong Z, Onrust R, O'Donnell M. 1993a. DNA polymerase III accessory proteins. III. holC and holD encoding chi and psi. J Biol Chem 268:11773–11778.

Xiao H, Dong Z, O'Donnell M. 1993b. DNA polymerase III accessory proteins. IV. Characterization of chi and psi. J Biol Chem 268:11779–11784.

Zhou M, Sandercock AM, Fraser CS, Ridlova G, Stephens E, Schenauer MR, Yokoi-Fong T, Barsky D, Leary JA, Hershey JW, Doudna JA, Robinson CV. 2008. Mass spectrometry reveals modularity and a complete subunit interaction map of the eukaryotic translation factor eIF3. Proc Natl Acad Sci USA 105:18139–18144.

Zhou M, Robinson CV. 2010. When proteomics meets structural biology. Trends Biochem Sci 35:522–529.

Editor: Michael M. Cox